IOP Publishing Smart Materials and Structures
Smart Mater. Struct. 25 (2016) 035007 (10pp) doi:10.1088/0964-1726/25/3/035007

Dynamically tuned magnetostrictive spring with electrically controlled stiffness

Justin J Scheidler[1], Vivake M Asnani[2] and Marcelo J Dapino[1]

[1] Department of Mechanical and Aerospace Engineering, The Ohio State University, Columbus, OH, 43210, USA
[2] Rotating and Drive Systems Branch, Materials and Structures Division, NASA Glenn Research Center, Cleveland, OH 44135, USA

E-mail: scheidler.8@osu.edu and dapino.1@osu.edu

Received 11 October 2015, revised 14 December 2015
Accepted for publication 17 December 2015
Published 8 February 2016

Abstract

This paper presents the design and testing of an electrically controllable magnetostrictive spring that has a dynamically tunable stiffness (i.e., a magnetostrictive Varispring). The device enables in situ stiffness tuning or stiffness switching for vibration control applications. Using a nonlinear electromechanical transducer model and an analytical solution of linear, mechanically induced magnetic diffusion, Terfenol-D is shown to have a faster rise time to stepped voltage inputs and a significantly higher magnetic diffusion cut-off frequency relative to Galfenol. A Varispring is manufactured using a laminated Terfenol-D rod. Further rise time reductions are achieved by minimizing the rod's diameter and winding the electromagnet with larger wire. Dynamic tuning of the Varispring's stiffness is investigated by measuring the Terfenol-D rod's strain response to dynamic, compressive, axial forces in the presence of sinusoidal or square wave control currents. The Varispring's rise time is <1 ms for 1 A current switches. Continuous modulus changes up to 21.9 GPa and 500 Hz and square wave modulus changes (dynamic ΔE effect) up to 12.3 GPa and 100 Hz are observed. Stiffness tunability and tuning bandwidth can be considerably increased by operating about a more optimal bias stress and improving the control of the electrical input.

Keywords: dynamic stiffness tuning, dynamic delta-E effect, Galfenol, Terfenol-D, vibration control

(Some figures may appear in colour only in the online journal)

1. Introduction

Magnetostrictive materials, such as Galfenol ($Fe_{1-x}Ga_x$, $0.13 \leqslant x \leqslant 0.29$) and Terfenol-D ($Tb_xDy_{1-x}Fe_y$, $x \approx 0.3$, $y \approx 2$), exhibit a bi-directional coupling between their magnetic and mechanical states, thereby providing actuation and sensing effects. The key advantages of magnetostrictive materials are noncontact operation, very high reliability [1], high bandwidth, and inherent active behavior. These materials also exhibit a reduction in their effective elastic moduli during magnetic domain rotation due to the superposition of purely elastic strain and magnetoelastic strain [2]. This effect enables the development of tunable stiffness components, which can be applied to a variety of vibration control problems. Variation in the Young's modulus $\boldsymbol{E}$ primarily results from two sources: a change in the magnetic boundary condition and a change in the bias magnetic field.

A change in the magnetic boundary condition from constant magnetic field (magnetically free condition) to constant magnetic flux density (magnetically blocked condition) causes an increase in the Young's modulus of magnetostrictive materials [3]. This is analogous to the increase in the Young's modulus of piezoelectric materials that results from a change in the electrical boundary condition from short circuit (electrically free condition) to open circuit (electrically blocked condition). This effect has been harnessed to develop piezoelectric semi-active vibration absorbers [4, 5] and high-speed stiffness-switching devices [6, 7]. In magnetostrictive materials, this effect has received limited attention, because a

change in the bias magnetic field can produce a significantly larger variation in the materials' Young's modulus [3].

The ΔE effect—changes in the quasi-static Young's modulus with changes in the bias magnetic field—has been well documented for Terfenol-D [8–12] and Galfenol [13–18]. When magnetic field strengths are limited (i.e., when the material cannot be saturated), the ΔE effect can be defined as

$$\Delta E = \frac{E_{H2} - E_{H1}}{E_{H2}}, \quad E_{H1} \geqslant E_{H2}, \tag{1}$$

where E_{H1} and E_{H2} are the Young's modulus at magnetic fields of $H1$ and $H2$, respectively [12]. Flatau *et al* [3], Pagliarulo *et al* [19], and Scheidler and Dapino [2, 20] used the ΔE effect to quasi-statically tune the resonant frequency of vibration absorbers. Kellogg and Flatau [11] measured the ΔE effect-induced change in resonant frequency of a Terfenol-D axial spring element that can be implemented as a parametric amplifier or for impedance matching. To realize in situ stiffness tuning, real-time tuning of the dynamic elastic properties via time-varying magnetic fields must be understood. A magnetostrictive spring with this capability facilitates many semi-active vibration control techniques, such as switched-stiffness vibration control [6, 21], structural tuning, high-speed tracking of disturbances, speed of sound modulation [22], and adaptive periodic structures [23]. Dynamic tuning has only been studied by Scheidler *et al* [24], who modeled and designed a magnetostrictive spring for high-speed, electrical tuning of its stiffness. Preliminary measurements of the influence of sinusoidal currents on the dynamic elastic response to sinusoidal compressive stresses were reported.

The electromechanical model of a magnetostrictive spring presented in [24] assumes linear constitutive behavior; this limits the model's application to cases for which the elastic modulus change is small. Additionally, design criteria based on magnetic diffusion did not consider the effect of laminating the magnetostrictive rod.

This paper addresses the limitations of [24] by (a) incorporating fully nonlinear stress and magnetic field dependence into the electromechanical model of the spring, (b) quantifying the magnetic diffusion response of laminated magnetostrictive rods by approximating them as solid rods having a reduced electrical conductivity, and (c) presenting the first measurement of the *dynamic* ΔE effect, i.e., the response of dynamic elastic moduli to switching of the bias magnetic excitation.

The manuscript is structured as follows. In section 2, the modeling and design of a magnetostrictive, variable-stiffness spring is presented, wherein the electromechanical response to arbitrary inputs is accurately quantified due to the inclusion of constitutive nonlinearities. This device is referred to as a magnetostrictive Varispring. Next, the experimental setup used to measure the dynamic elastic response of the Varispring to electrical, stiffness-control signals is described in section 3. Section 4 presents measurements of dynamic elastic modulus tuning, including the dynamic ΔE effect. Section 5 contains a discussion of a key characteristic of the Varispring and methods to improve its performance.

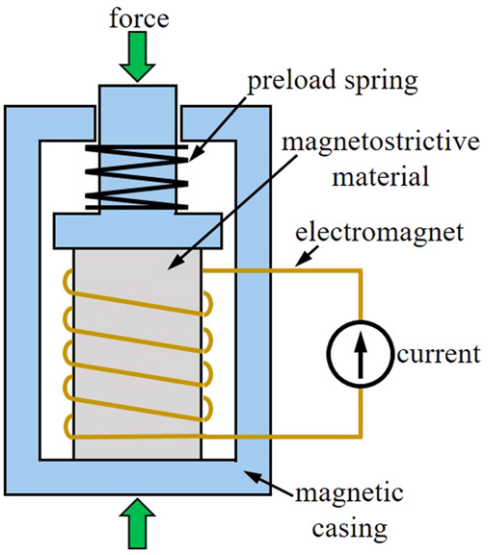

Figure 1. Schematic of the magnetostrictive Varispring.

2. Modeling and design of the magnetostrictive Varispring

The magnetostrictive Varispring was designed to operate as an axial spring element that has an electrically controllable and dynamically tunable stiffness. A schematic of the device is depicted in figure 1. The contained magnetostrictive rod was magnetically biased and excited using a current-controlled electromagnet and mechanically biased such that small motions did not appreciably affect the preload. The rod and electromagnet are enclosed by a magnetic casing that was designed to provide a uniform, axial magnetic state in the magnetostrictive rod. The Varispring was designed for a test rig at NASA Glenn Research Center that needed a real-time tunable stiffness element; for this application, requirements were set for the Varispring's overall geometry (50 mm diameter, 105 mm height), the axial stiffness of the magnetostrictive rod (500 N μm^{-1}), and the maximum applied dynamic force (1000 N). Therefore, the length of the magnetostrictive rod was selected as the independent design variable, with which the rod's diameter and other geometric parameters were directly evaluated from the constraints [24].

2.1. Electromechanical modeling of the Varispring

The electromechanical response of a magnetostrictive transducer operated sufficiently below its first mechanical resonant frequency can be modeled as

$$F(s) = K^H s^{-1} \Delta v(s) - GI(s), \tag{2}$$

$$V(s) = G\Delta v(s) + (L^S s + R_{\text{coil}}) I(s), \tag{3}$$

where s is the Laplace parameter, F represents the force in the magnetostrictive rod (tension positive), Δv denotes the relative velocity of the ends of the rod, I and V are the current in and voltage applied to the electromagnet, respectively, and R_{coil} is the electromagnet's resistance [25, 26]. Constitutive nonlinearities are incorporated by

retaining the magnetic field H and stress T dependence of the electrical and mechanical properties: the rod's axial stiffness at constant magnetic field K^H, and the transducer's inductance at constant strain L^S and electromechanical coupling coefficient G,

$$K^H(H, T) = E^H(H, T)A_{\text{rod}}l_{\text{rod}}^{-1}, \tag{4}$$

$$L^S(H, T) = N^2A_{\text{coil}}(\mu^T(H, T) - d(H, T)^2E^H(H, T))l_{\text{coil}}^{-1}, \tag{5}$$

$$G(H, T) = d(H, T)E^H(H, T)NA_{\text{rod}}l_{\text{coil}}^{-1}. \tag{6}$$

In (4)–(6), μ^T, d, E^H, l_{rod}, and A_{rod} denote the magnetic permeability at constant stress, piezomagnetic coefficient, Young's modulus at constant field, length, and cross-sectional area of the magnetostrictive rod, respectively, and N, l_{coil}, and A_{coil} are the number of windings in, axial length of, and cross-sectional area enclosed by the electromagnet, respectively. In this paper, the stress- and field-dependent material properties were calculated using 1D, anhysteretic formulations of the nonlinear, fully coupled constitutive models of Galfenol and Terfenol-D developed by Evans and Dapino [27, 28] and Chakrabarti and Dapino [29]. The models were optimized to existing measurements [12, 30]. To improve computational efficiency, these models were implemented as interpolation functions with very fine input grids.

Assuming that magnetic flux leakage and the magnetic reluctance of the Varispring's flux return path are negligible, the magnetic field in the magnetostrictive rod is $H(s) = NI(s)/l_{\text{coil}}$. For a mechanical load of mass m, (2) and (3) can be combined with the expression for $H(s)$ to quantify the field generated in the magnetostrictive rod by an applied voltage

$$H(s) = \frac{N}{l_{\text{coil}}} \times \frac{ms^2 + K^H}{L^S ms^3 + R_{\text{coil}}ms^2 + (G^2 + L^S K^H)s + R_{\text{coil}}K^H}V(s), \tag{7}$$

where the dependence of K^H, L^S, and G on H and T was dropped from the notation for compactness. This model does not incorporate eddy current effects and is thus more accurate for magnetostrictive rods operating below their magnetic diffusion cut-off frequency.

To maintain compressive loading of the magnetostrictive rod during dynamic operation, the Varispring is operated at a moderate compressive mechanical bias for which the rod's zero-field Young's modulus is nearly saturated (i.e., the stiff state). From this bias, the Varispring's stiffness is decreased by increasing the field from zero to a tuning field H_{soft}. To approximate the time required to switch the Varispring's stiffness from the stiff state to the soft state, the rise time to reach H_{soft} from zero in response to a voltage step was calculated for $m = 2$ kg and $l_{\text{coil}} = l_{\text{rod}}$. Rise times were calculated using the minimum number of windings N_{min} needed to generate the tuning field with 95% of the maximum current I_{max} for a given wire gauge, i.e., $N_{\text{min}} = H_{\text{soft}}l_{\text{coil}}/(0.95I_{\text{max}})$. In this way, the effective electrical inductance was minimized for each design case.

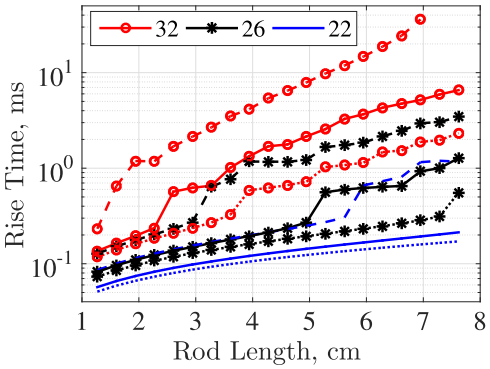

Figure 2. Rise time to reach H_{soft} from $H = 0$ in response to a 250 V step voltage input to electromagnets wound with 32, 26, and 22 AWG wire; Galfenol, ΔE_{max} (—); Terfenol-D, ΔE_{max} (- - -); and Terfenol-D, ΔE_{eq} (·····).

The rise times for Galfenol- and Terfenol-D-based Varisprings are depicted in figure 2. Three cases are considered: (a) Galfenol, maximum Young's modulus change ($\Delta E_{\text{max}} \approx 30$ GPa, $H_{\text{soft, max}} = 11\,\text{kA m}^{-1}$) [18], (b) Terfenol-D, near maximum Young's modulus change ($\Delta E_{\text{max}} \approx 90$ GPa, $H_{\text{soft, max}} = 80\,\text{kA m}^{-1}$) [12], and (c) Terfenol-D, near maximum (field-limited) Young's modulus change ($\Delta E_{\text{eq}} \approx 30$ GPa, $H_{\text{soft}} = 35\,\text{kA m}^{-1}$) [12]. The bias stress T_{bias} for all three cases is -42 MPa.

In general, the rise time decreases with the magnetostrictive rod's length, because A_{rod} decreases with its length to maintain a given nominal stiffness, which reduces A_{coil} and thus the blocked inductance. The rise time also decreases with the wire gauge, because electromagnets wound using larger wire diameters can generate H_{soft} with fewer windings due to their larger I_{max}. This reduces the coil's inductance, but at the expense of higher electrical power demands [24]. Maximal stiffness tuning of a Terfenol-D-based Varispring is appreciably slower than that of a Galfenol-based Varispring despite Galfenol's significantly higher magnetic permeability (and thus blocked inductance) due to the larger tuning field that must be generated. However, for the same change in Young's modulus, Terfenol-D provides a slightly faster response.

2.2. Effect of dynamic stress on bias magnetic fields

When magnetostrictive rods are subjected to constant surface magnetic fields and dynamic axial stresses, internal eddy currents are generated, which, if the forcing frequency exceeds a diffusion cut-off frequency ω_c, significantly suppress the material's active response [31]. Scheidler and Dapino [31] analytically derived this cut-off frequency for linear constitutive regimes

$$\omega_c = 4.3393(\mu^T\sigma R^2)^{-1}, \tag{8}$$

where R and σ are the radius and electrical conductivity of the rod, respectively. Since the Varispring is designed to operate under small amplitude dynamic stresses to maximize the stiffness variation between two bias field states, the linearity assumption is valid for dynamic loading about each bias field.

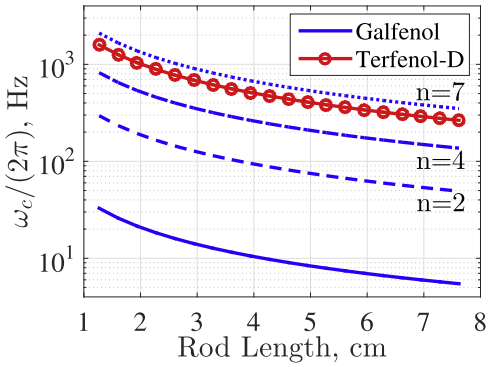

Figure 3. Mechanically induced magnetic diffusion cut-off frequency of 6.3 mm diameter solid Terfenol-D, solid Galfenol, and laminated (with n laminates) Galfenol rods[3]; Terfenol-D: $\sigma = 1.72$ S μm^{-1}[32], $\mu^T/\mu_0 = 9.4$; Galfenol: $\sigma = 2.15$ S μm^{-1}[18, 33], $\mu^T/\mu_0 = 240$[18].

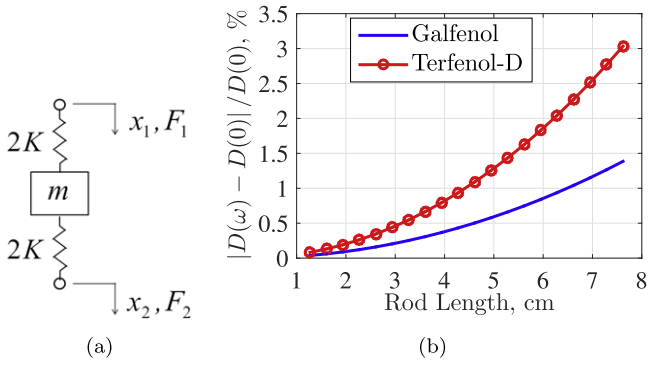

Figure 4. Effect of internal mass on the magnetostrictive rod's dynamic stiffness, (a) lumped parameter model and (b) percent change in the dynamic stiffnesses from their static values[4]; Terfenol-D: $E^H_{\min} = 18$ GPa, $\rho = 9250$ kg m^{-3}; Galfenol: $E^H_{\min} = 33$ GPa, $\rho = 7870$ kg m^{-3}.

Figure 3 depicts the diffusion cut-off frequency of 6.3 mm diameter Galfenol and Terfenol-D rods operating about a moderate compressive bias stress (e.g., about −25 to −50 MPa) and the worst-case bias field (that which maximizes μ and nearly minimizes E). The magnetic permeability of each rod was analytically calculated using the aforementioned constitutive models.

In general, the cut-off frequencies decrease with increases in the rod's length, because the rod's diameter must increase accordingly to maintain a given stiffness. The cut-off frequency of the Terfenol-D rod is nearly two orders of magnitude greater than that of the Galfenol rod. Thus, the cut-off frequency of laminated Galfenol rods were also calculated by approximating a laminated rod as a solid rod with an effective electrical conductivity

$$\sigma_{\text{eff}} = \sigma/(n+1)^2, \tag{9}$$

where n is the number of laminates [34]. For the properties considered, the Galfenol rod must be laminated with 7 or more laminates for its cut-off frequency to exceed that of the solid Terfenol-D rod. Although not considered here, lamination also softens the rod due to the presence of adhesive layers that have a modulus of only 0.86 GPa; due to the axial stiffness constraint, this, in turn, slightly affects the cut-off frequency of the rod through its geometry.

2.3. Effect of internal mass on dynamic stiffness

The mass of a structure influences its dynamic stiffness, particularly at higher frequencies. The objective of this study was to develop a spring element having a controllable stiffness. Changes in stiffness due to mass effects reduce the controllability and introduce frequency dependence. Consequently, the rod was designed to minimize these effects.

Below the first mechanical resonance, the effect of internal mass $m = \rho A_{\text{rod}} l_{\text{rod}}$ on the dynamic stiffness D of the magnetostrictive rod can be approximated using the lumped parameter model shown in fig. 4(a), where ρ is the density. After assuming harmonic motion, the application of Newton's second law to this model gives

$$\begin{bmatrix} F_1 \\ F_2 \end{bmatrix} = \begin{bmatrix} D_{11}(\omega) & D_{12}(\omega) \\ D_{21}(\omega) & D_{22}(\omega) \end{bmatrix} \begin{bmatrix} x_1 \\ x_2 \end{bmatrix}, \tag{10}$$

where the driving-point stiffnesses D_{11}, D_{22} and cross-point stiffnesses D_{12}, D_{21} are

$$\begin{aligned} D_{11}(\omega) = D_{22}(\omega) &= \frac{2K(2K - m\omega^2)}{4K - m\omega^2}, \\ D_{12}(\omega) = D_{21}(\omega) &= \frac{-4K^2}{4K - m\omega^2}, \end{aligned} \tag{11}$$

where x denotes the displacement of the rod's ends, K is the axial stiffness of the rod, and ω is the angular forcing frequency. Figure 4(b) depicts the absolute value of the percent change in the driving-point and cross-point stiffnesses of Galfenol and Terfenol-D rods for worst-case conditions (i.e., the maximum frequency, 1000 Hz, and minimum expected Young's modulus of the materials $E^H_{\min}$). The effect of internal mass on the dynamic stiffness of a Terfenol-D rod is nearly double that of a Galfenol rod due to Terfenol-D's smaller $E^H_{\min}$ and higher density; however, the effect is small in both cases for the parameters considered.

2.4. Design of the Varispring

A prototype Varispring utilizing Terfenol-D was manufactured, because the use of Terfenol-D provides a significantly higher diffusion cut-off frequency and quasi-static Young's modulus variation [12, 18] for rise times comparable to those of Galfenol-based Varisprings. As supplied by Etrema Products, Inc., the Terfenol-D ($Tb_{0.3}Dy_{0.7}Fe_{1.92}$) rod includes 0.762 mm (0.030 in) thick laminations separated by adhesive layers of about 0.048 mm (0.0019 in) thickness to further improve its dynamic performance. The elastic modulus of the adhesive is 862 MPa. A length of 2.401 cm (0.9453 in) was selected to balance the improved performance of shorter rods with the need to attach sensors. If sensors were

[3] Note that the dependence of ω_c on l_{rod} results from the axial stiffness constraint.

[4] The driving-point and cross-point stiffnesses overlap.

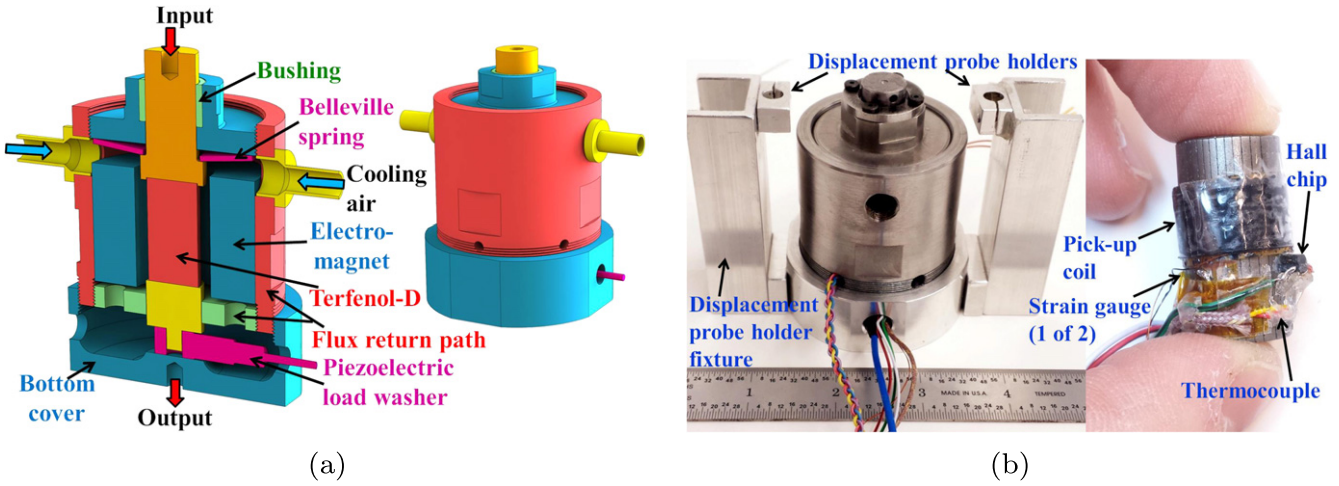

Figure 5. (a) CAD model of the prototype Varispring and (b) manufactured Varispring with capacitive displacement probe holder fixture attached (left) and Terfenol-D rod with sensors installed (right) [24] Copyright 2015 SPIE[5].

not required, a shorter rod could have been used; however, the minimum length would still be bounded by the size of the electromagnet needed to generate a given magnetic field and by the desired maximum stress. A diameter of 1.271 cm (0.5005 in) provided the desired maximum axial stiffness of the rod. For the chosen geometry of the Terfenol-D rod, the effect of its internal mass on its dynamic stiffness is negligible.

During experimental testing of the Varispring, the mechanical preload was applied by a load frame. When the device is used in a vibration control application, the preload can be generated by a softening Belleville spring operated near its maximum deflection to minimize variations in the preload during operation [11]. A century spring CDM-401413 Belleville spring was included in the Varispring's design (as shown in the following CAD model), but it was not used during the reported testing, because the load frame could more directly apply the preload.

Figure 5(a) depicts a CAD model of the prototype Varispring. The central load path—from the input through the Terfenol-D rod and along the device's cylindrical axis to the output—acts as an elastic member (i.e., a spring) with a variable stiffness. In this work, stiffness was modulated via controlled changes in the electromagnet's current, which almost proportionally altered the axial magnetic field applied to the Terfenol-D. The field versus current response exhibited some nonlinearity due to Terfenol-D's stress- and magnetic field-dependent magnetic permeability, as detailed by Atulasimha *et al* [14]. The electromagnet was wound using 519 turns of 22 AWG wire and was held together by Duralco 4525 epoxy having a thermal conductivity of 1.875 W/(m °K). The magnetic flux return path was designed using magnetostatic finite element simulations to ensure that Terfenol-D's magnetic state is nearly uniform when magnetic diffusion and internal mechanical dynamics are negligible. A sleeve bushing isolates the flux return path from forces applied to the central load path. Using equations given by Scheidler *et al* [18], the inertial force error at 1000 Hz for this design is about 0.2%. During testing, the Varispring was aligned to the load frame using the blind holes on its ends.

As detailed by Scheidler *et al* [18, 35], the inertial force of vibrating masses located in-between the force transducer and the magnetostrictive rod cause errors in the measurement of the dynamic force in the rod. This error was kept below the ASTM-recommended tolerance of 0.5% [36] by measuring this dynamic force using a piezoelectric load washer nearly collocated with the rod. The dynamic, axial force was measured using a Kistler 9001A piezoelectric load washer.

The manufactured prototype and instrumented Terfenol-D rod are depicted in figure 5(b). The total displacement of the Varispring, i.e., the relative displacement between the bottom of the Varispring and a cylindrical target (shown in figure 6) that mounted to the top of the device, was measured using MicroSense 8810 capacitive displacement probes.

3. Experimental setup

Mechanical testing of the prototype Varispring was conducted using an MTS 831.50 high frequency load frame. The axial strain at the surface of the Terfenol-D rod was measured using a pair of Vishay Micro-Measurements EA-06-250BF-350/L strain gauges, which were bonded on opposite sides of the rod and wired in series to cancel bending strains and the electromagnetic noise induced in the gauges due to the time-varying magnetic flux density in the rod [18]. A lake shore model 480 fluxmeter and custom pick-up coil were utilized to measure the magnetic flux density in the rod. An Allegro A1302ELH Hall chip was used to measure the axial magnetic field at the surface of the Terfenol-D rod. The rod's temperature was monitored with a Type K thermocouple to ensure that temperature increases above the 25 °C ambient were <3 °C.

[5] The air hose fittings are not shown in the picture. The passive structural components are 1018 steel, except for the Belleville spring (high carbon steel), bushing (Rulon J), air hose fittings (brass), and bottom cover (Al 7075).

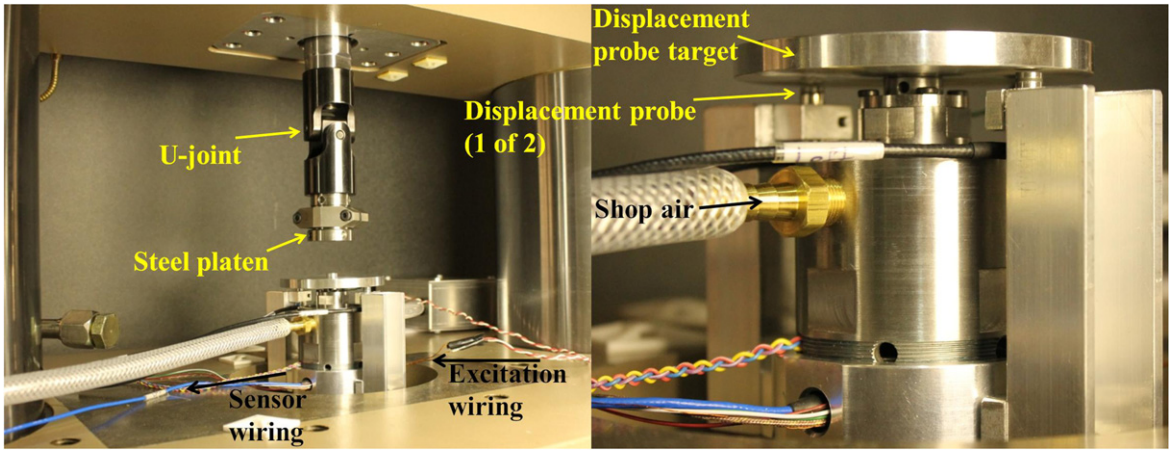

Figure 6. Experimental setup (the compression spring used to improve the force control during dynamic stiffness tuning tests is not shown) [24]. Copyright 2015 SPIE.

The electromagnet was excited by a Techron LVC 5050 linear amplifier operated in current control mode. The amplifier's voltage monitor measured the supply voltage. However, the supply current was calculated from the voltage drop across a 0.1 ± 0.001 Ohm, 15 W Leeds and Northrup Co. resistor connected in series with the Varispring, because the current monitor exhibited an erroneous offset that changed throughout the experiment. The sensors were calibrated as detailed by Scheidler *et al* [18], except for the pick-up coil, which was calibrated by measuring the static magnetic field generated in air between the poles of a large electromagnet using the pick-up coil and calibrated Hall sensor. The calibration factor of the pick-up coil (NA) was then scaled to correct for the presence of glue layers in the laminated Terfenol-D rod

$$(NA)_{\text{corrected}} = (NA)A_{\text{solid}}/A_{\text{lam}}, \tag{12}$$

where A_{lam} and A_{solid} respectively are the cross-sectional areas of Terfenol-D in the laminated rod and a solid rod of the same diameter. Measurement signals were phase aligned in post processing by correcting for the phase response of the conditioning electronics [18].

The experimental setup is shown in figure 6. When dynamic forces were directly applied to the displacement probe target by the steel platen, the load frame's force control system performed poorly due to the Varispring's large, high-speed stiffness changes (a disturbance to the force control system). This resulted in a highly nonlinear applied force that significantly deviated from the sinusoidal command signal, particularly when the current frequency was high. Consequently, during dynamic stiffness tuning experiments, a $1.3\ \text{N}\ \mu\text{m}^{-1}$ compression spring (less than 1% of the Varispring's stiffness) was inserted between the platen and target to act as a mechanical low-pass filter to attenuate the disturbance; the improved force control, depicted in figure 7, adequately preserves the sinusoidal shape of the command signal over the frequency range of interest (up to 1 kHz). However, due to the large motion of the steel platen that resulted, the displacement probes were removed from the experimental setup during dynamic stiffness tuning tests to prevent the possibility of damaging the probes. Thus, the Varispring's stiffness could not be calculated; instead, the strain response and Young's modulus of the Terfenol-D rod are used to study the Varispring's time-varying elastic state.

4. Measurements of dynamic Young's modulus tuning

First, the quasi-static sensing response of the Terfenol-D rod was measured under constant current over the stress range of interest. The Young's modulus of the rod, shown in figure 8, was calculated by differentiating 4th order polynomials that were fit to 0.75 MPa wide sections of each half of the hysteretic responses [18]. When the maximum current, and thus magnetic field, is limited (e.g., to prevent excessive rise times), a larger ΔE effect can be realized at higher compressive bias stresses. At the bias stress for which the Varispring was designed (−25 MPa), the maximum change in the minor loop Young's modulus (51 GPa) occurred when the current was increased from 0 A to 3.08 A. However, to prevent full compression of the required isolation spring, the bias was constrained to >-6 MPa. As evidenced by figure 8, this reduced the achievable Young's modulus variation during dynamic tuning experiments, because the current could not be increased above 5 A. Also, due to the change in bias stress, current increases stiffened the Varispring rather than softening it as originally intended.

Dynamic tuning of the Varispring's elastic state was conducted in two stages. First, the stiffness was continuously varied by applying a 1–1000 Hz sinusoidal current having a nominal amplitude of 1.50 A and bias of 1.56 A. Second, high-speed switching of the stiffness was realized via a 1 to 500 Hz square wave current having a bias of 1.56 A. To prevent instability of the amplifier's current control system, the nominal amplitude of the square wave current was reduced to 0.50 A. In each case, the Varispring was excited with a 2.00–5.80 MPa amplitude, 25 Hz sinusoidal stress.

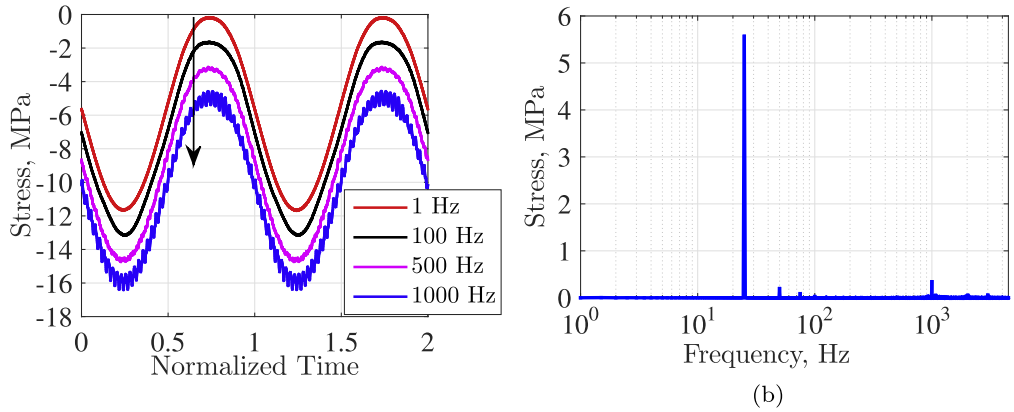

Figure 7. Force control performance when using a soft compression spring; 5.80 MPa amplitude, 25 Hz sinusoidal forcing and 1.5 A amplitude sinusoidal current: (a) effect of current frequency[6] (frequency increases in the direction of the arrow) and (b) fast Fourier transform of the 1000 Hz current response.

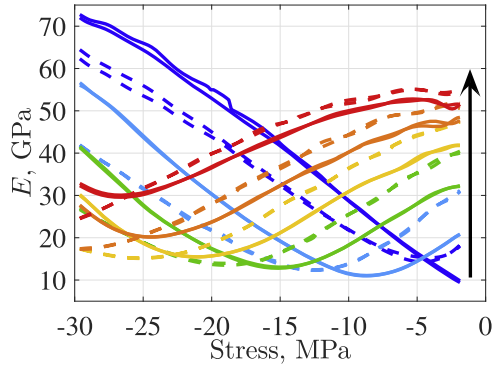

Figure 8. Quasi-static Young's modulus of the laminated Terfenol-D rod at constant currents of 0, 0.909, 1.72, 2.59, 3.52, and 4.82 A; bias current increases from blue to red (direction shown by the arrow); stress increasing (—), stress decreasing (- - -), two cycles shown.

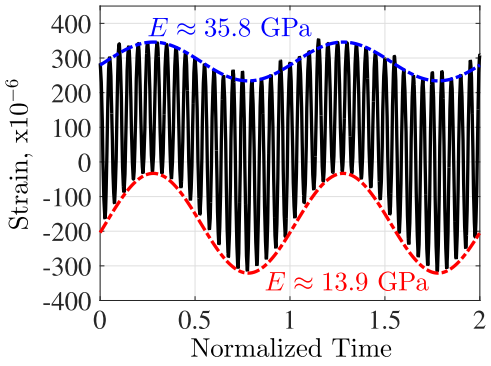

Figure 9. Strain response of the Terfenol-D rod to a 500 Hz sinusoidal current and a 25 Hz, 2.00 MPa amplitude stress with −5.90 MPa bias.

The strain response of the Terfenol-D rod inside the prototype Varispring to a 500 Hz sinusoidal current is depicted in figure 9. Both the stiffness change and the current induced actuation strain introduce harmonic content at the frequency of the current. The blue and red annotations respectively indicate the approximate Young's modulus at the maximum and minimum current ($E_{I\,\max}$ and $E_{I\,\min}$), which, at the intended operating bias, would correspond to the low and high modulus, respectively. However, figure 8 suggests that at a −5.90 MPa bias, the minimum modulus occurs for a small, but nonzero current between 0 and 0.909 A. Consequently, $\Delta = E_{I\,\max} - E_{I\,\min}$ increases when the current amplitude is slightly reduced; this is shown in table 1, which gives the current amplitude and approximate moduli for each testing condition. Also shown is the absolute value of the ΔE effect, where E_{H1} is taken as $E_{I\,\max}$, and E_{H2} is taken as $E_{I\,\min}$. The amplifier did not maintain a consistent current amplitude, despite using the same current control voltage for each case; with this caveat, the Terfenol-D rod is stiffer for a smaller stress amplitude, as also observed by Kellogg and Flatau [12]. The rod's modulus tunability is roughly maintained through 500 Hz, but is degraded at 1 kHz. This primarily results from a considerable reduction in the applied current amplitude. Magnetic diffusion in the flux return path may also contribute to this reduction, although this was not investigated.

The current control performance during testing of the dynamic ΔE effect (i.e., square wave elastic modulus tuning) is depicted in figure 10. Even though the amplifier's current control system was tuned according to the manufacturer's suggestions, a significant amount of overshoot is observed. The settling time of this overshoot is about 2 ms; thus, a 500 Hz (2 ms period) square wave current could not be produced and the 500 Hz strain response is not shown.

The strain response of the Terfenol-D rod inside the prototype Varispring to 1 and 100 Hz square wave currents is illustrated in figure 11. In figure 11(a), the discrete change in Young's modulus is distinguished by the strain amplitude at each current state. As seen in the inset of figure 11(b), the strain response exhibits an overshoot akin to the current overshoot. This implies that the Varispring's rise time is <1 ms, as predicted by the nonlinear electromechanical model in section 2.1. The approximate Young's moduli of the rod at the high and low current states are tabulated in table 2 for

[6] To improve visualization, the curves were successively shifted downward by 1.5 MPa in post-processing starting with the 100 Hz curve.

Table 1. Approximate Young's moduli (in units of GPa) of the Terfenol-D rod at the maximum and minimum current for a bias stress of -5.90 MPa and different sinusoidal current frequencies and stress amplitudes.

	2.00 MPa					5.80 MPa				
Freq., Hz	$\|I\|$, A	$E_{I\,\min}$	$E_{I\,\max}$	Δ	$\|\Delta E\|$, %	$\|I\|$, A	$E_{I\,\min}$	$E_{I\,\max}$	Δ	$\|\Delta E\|$, %
1	1.50	25.5	42.1	16.6	65.1	1.29	17.8	37.8	20.0	112
100	1.50	15.0	34.5	19.5	130	1.57	14.4	28.8	14.4	100
500	1.21	13.9	35.8	21.9	158	1.28	15.3	29.8	14.5	94.8
1000	1.07	22.0	26.8	4.80	21.8	1.07	19.9	22.8	2.90	14.6

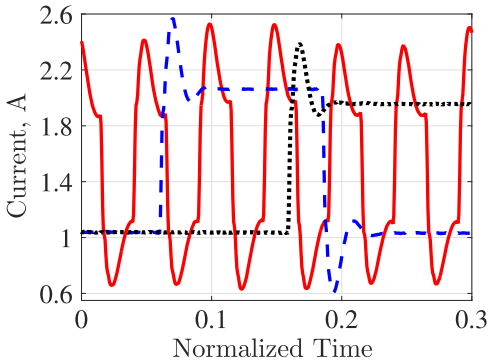

Figure 10. Current control performance; 25 Hz, 4.00 MPa amplitude sinusoidal forcing and square wave current frequencies of 50 Hz (·····), 100 Hz (- - -), and 500 Hz (—).

each testing condition. The dynamic ΔE effect is fairly consistent from 1 Hz through 100 Hz and for the two stress amplitudes. This consistency between the two stress amplitudes is supported by quasi-static measurements by Kellogg and Flatau [12], who showed that Δ is almost independent of stress amplitude when Terfenol-D operates far away from saturation; if the current amplitude had been increased such that the Terfenol-D rod operated close to saturation at one of the two current states, then a larger Δ would be expected for the 2.00 MPa case.

5. Discussion

To improve the Varispring's stiffness tunability, the device can be operated about a higher bias stress, which can be realized by using a compression spring with greater travel or by generating some of the bias with an internal Belleville spring. During stiffness switching, stiffness tunability and tuning bandwidth can be increased by optimizing the current control. Alternatively, improvements may be possible by using voltage control or by low-pass filtering the square wave current to reduce its harmonic content. The use of voltage control should prevent instability and overshoot caused by the amplifier, but it would complicate the control of E due to the strong frequency dependence of the Varispring's electrical impedance. Magnetic field control (as opposed to current control) would provide better control over E. However, field control was not studied, because of the difficulty in implementing it at high frequencies [18].

A fundamental characteristic of stiffness tuning via changes in the applied magnetic field (i.e., using the ΔE effect) is the actuation strain that simultaneously occurs. When the actuation strain cannot be accounted for, it may limit the Varispring's effectiveness in a variety of applications. In such cases, the Young's modulus of the Terfenol-D rod (and hence the Varispring's stiffness) can be tuned by changing the magnetic boundary condition of the rod. This can be accomplished by connecting an inductive shunt to the Varispring's electromagnet rather than an electrical excitation. This technique provides a considerably smaller change in E [3]. However, the use of negative inductance circuits can significantly increase the change [37]. This approach requires a synthetic inductance circuit to achieve negative inductance or to continuously tune the stiffness.

6. Summary and Conclusions

In this paper, an electrically controllable magnetostrictive spring capable of dynamic stiffness tuning (i.e., a magnetostrictive Varispring) was designed, manufactured, and tested. The design was based on (a) a nonlinear electromechanical transducer model, (b) an analytical solution of linear, mechanically induced magnetic diffusion, and (c) the effect of internal mass on the magnetostrictive material's dynamic stiffness. Terfenol-D has a much larger potential for Young's modulus tuning than Galfenol. The modeling results show that for an equal modulus change, Terfenol-D provides a slightly faster rise time to control inputs. A laminated Terfenol-D rod was selected as the active material for this reason and for its significantly higher magnetic diffusion cut-off frequency. To decrease the rise time, the electromagnet was wound with relatively large wire (22 AWG) and the rod's length (and thus its diameter) was minimized.

Dynamic tuning of the Varispring's stiffness was investigated by measuring the Terfenol-D rod's strain response to dynamic, compressive, axial forces in the presence of time-varying current inputs. Continuous and discrete Young's modulus tuning were realized via sinusoidal and square wave currents, respectively. To achieve an acceptable level of force control, a soft compression spring was added to the load path to mechanically isolate the force control from the high speed changes in the Varispring's stiffness. This change in the experimental setup prevented the measurement of displacement and so Young's modulus was used as an alternative

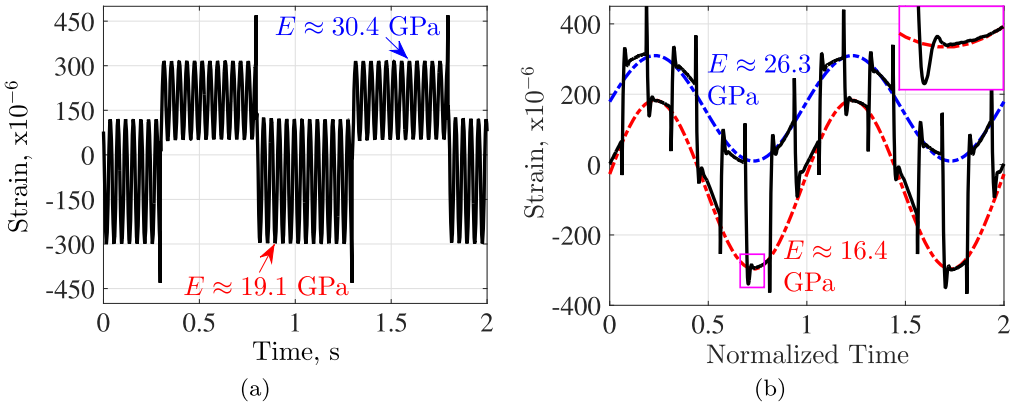

Figure 11. Strain response of the Terfenol-D rod to a (a) 1 Hz and (b) 100 Hz square wave current and a 25 Hz, 4.00 MPa amplitude stress with −5.90 MPa bias.

Table 2. Approximate Young's moduli (in units of GPa) of the Terfenol-D rod at the high current and low current states for a bias stress of −5.90 MPa and different square wave current frequencies and stress amplitudes.

	2.00 MPa					4.00 MPa				
Freq.,Hz	$\|I\|$, A	$E_{I\,\min}$	$E_{I\,\max}$	Δ	$\|\Delta E\|$, %	$\|I\|$, A	$E_{I\,\min}$	$E_{I\,\max}$	Δ	$\|\Delta E\|$, %
1	0.55	22.9	32.8	9.90	43.2	0.55	19.1	30.4	11.3	59.2
10	0.57	22.3	31.2	8.90	39.9	0.51	19.3	30.0	10.7	55.4
50	0.50	21.4	30.2	8.80	41.1	0.49	17.0	29.3	12.3	72.4
100	0.49	16.8	29.1	12.3	73.2	0.49	16.4	26.3	9.90	60.4

metric of performance. The spring also had a relatively low maximum force, which reduced the maximum compressive bias and consequently reduced the attainable Young's modulus variation. Nevertheless, continuous modulus changes up to 21.9 GPa and 500 Hz were observed for current amplitudes up to 1.5 A. Square wave modulus changes (dynamic ΔE effect) up to 12.3 GPa and 100 Hz were observed for current amplitudes up to 0.5 A. Instability and overshoot in the controlled square wave current prevented measurement at higher control frequencies and amplitudes. The rise time of the Varispring was <1 ms. A discussion of the unintended actuation that accompanied the stiffness changes as well as methods to improve the Varispring's performance was then presented.

This Varispring has broad application to vibration control and enables a variety of in situ stiffness control techniques, such as stiffness switching and structural tuning. Possible areas of future work include quantifying the durability of the device, improving the current control system, demonstrating the device's vibration control capabilities, studying the influence of the unintended actuation and comparing the merits of dynamic stiffness tuning via magnetic field changes and magnetic boundary condition changes.

Acknowledgments

This work was supported by the NASA Aeronautics Scholarship Program (grant # NNX14AE24H). Additional support was provided by NASA's Revolutionary Vertical Lift Technology (RVLT) Project and the member organizations of the Smart Vehicle Concepts Center (www.SmartVehicleCenter.org) a National Science Foundation Industry/University Cooperative Research Center.

References

[1] Prajapati K, Greenough R D and Wharton A 1997 Magnetic and magnetoelastic response of stress cycled Terfenol-D *J. Appl. Phys.* **81** 5719–21
[2] Scheidler J J and Dapino M J 2013 Nonlinear dynamic modeling and resonance tuning of Galfenol vibration absorbers *Smart Mater. Struct.* **22** 085015
[3] Flatau A B, Dapino M J and Calkins F T 2000 High bandwidth tunability in a smart vibration absorber *J. Intell. Mater. Syst. Struct.* **11** 923–9
[4] Cunefare K A, De Rosa S, Sadegh N and Larson G 2000 State-switched absorber for semi-active structural control *J. Intell. Mater. Syst. Struct.* **11** 300–10
[5] Davis C L and Lesieutre G A 2000 An actively tuned solid-state vibration absorber using capacitive shunting of piezoelectric stiffness *J. Sound Vib.* **232** 601–17
[6] Clark W W 2000 Vibration control with state-switched piezoelectric materials *J. Intell. Mater. Syst. Struct.* **11** 263–71
[7] Corr L R and Clark W W 2002 Comparison of low-frequency piezoelectric switching shunt techniques for structural damping *Smart Mater. Struct.* **11** 370
[8] Clark A E and Savage H T 1975 Giant magnetically induced changes in the elastic moduli in Tb0.3Dy0.7Fe2 *IEEE Trans. Sonics Ultrason.* **22** 50–51

[9] Savage H T, Clark A E and Powers J 1975 Magnetomechanical coupling and δ E effect in highly magnetostrictive rare Earth-Fe 2 compounds *IEEE Trans. Magn.* **11** 1355–7
[10] Moffett M B, Clark A E, Wun-Fogle M, Linberg J, Teter J P and McLaughlin E A 1991 Characterization of Terfenol-D for magnetostrictive transducers *J. Acoust. Soci. Am.* **89** 1448–55
[11] Kellogg R and Flatau A 2004 Wide band tunable mechanical resonator employing the δ E effect of Terfenol-D *J. Intell. Mater. Syst. Struct.* **15** 355–68
[12] Kellogg R and Flatau A 2008 Experimental investigation of Terfenol-D's elastic modulus *J. Intell. Mater. Syst. Struct.* **19** 583–95
[13] Kellogg R A, Flatau A B, Clark A E, Wun-Fogle M and Lograsso T A 2005 Quasi-static transduction characterization of Galfenol *J. Intell. Mater. Syst. Struct.* **16** 471
[14] Atulasimha J, Flatau A B and Kellogg R A 2006 Sensing behavior of varied stoichiometry single crystal Fe–Ga *J. Intell. Mater. Syst. Struct.* **17** 97–105
[15] Wun-Fogle M, Restorff J B and Clark A E 2009 Soft and hard elastic moduli of Galfenol transduction elements *J. Appl. Phys.* **105** 07A923
[16] Datta S, Atulasimha J, Mudivarthi C and Flatau A B 2010 Stress and magnetic field-dependent Young's modulus in single crystal iron–gallium alloys *J. Magn. Magn. Mater.* **322** 2135–44
[17] Restorff J B, Wun-Fogle M and Summers E 2011 Hysteresis, $d*_{33}$ and d_{33} of $Fe_{81.6}Ga_{18.4}$ textured polycrystals *J. Appl. Phys.* **109** 07A922
[18] Scheidler J J, Asnani V M and Dapino M J 2016 Dynamic characterization of Galfenol ($Fe_{81.6}Ga_{18.4}$) *NASA Report* NASA/TP-2016-218754
[19] Pagliarulo P, Kuhnen K, May C and Janocha H 2004 Tunable magnetostrictive dynamic vibration absorber *Proc. 9th Int. Conf. on New Actuators* 367–370
[20] Scheidler J J and Dapino M J 2014 Stiffness tuning of FeGa structures manufactured by ultrasonic additive manufacturing *Proc. SPIE* **9059** 905907
[21] Ramaratnam A and Jalili N 2006 A switched stiffness approach for structural vibration control: theory and real-time implementation *J. Sound Vib.* **291** 258–74
[22] Ruzzene M and Baz A 2000 Attenuation and localization of wave propagation in periodic rods using shape memory inserts *Smart Mater. Struct.* **9** 805–16
[23] Asiri S, Baz A and Pines D 2005 Periodic struts for gearbox support system *J. Vib. Control* **11** 709–21
[24] Scheidler J J, Asnani V M and Dapino M J 2015 Design and testing of a dynamically tuned magnetostrictive spring with electrically controlled stiffness *Proc. SPIE* **9433** 94330F
[25] Hunt F V 1954 *Electroacoustics: The Analysis of Transduction, and its Historical Background* (Acoustical Society of America) (Cambridge, MA: Harvard University Press)
[26] Engdahl G (ed) 2000 *Handbook of Giant Magnetostrictive Materials* (San Diego, CA: Academic)
[27] Evans P G and Dapino M J 2010 Efficient magnetic hysteresis model for field and stress application in magnetostrictive Galfenol *J. Appl. Phys.* **107** 063906
[28] Tari H, Scheidler J J and Dapino M J 2015 Robust solution procedure for the discrete energy-averaged model on the calculation of 3D hysteretic magnetization and magnetostriction of iron-gallium alloys *J. Magn. Magn. Mater.* **384** 266–75
[29] Chakrabarti S and Dapino M J 2012 Fully coupled discrete energy-averaged model for Terfenol-D *J. Appl. Phys.* **111** 054505
[30] Scheidler J J 2015 Static and dynamic delta E effect in magnetostrictive materials with application to electrically tunable vibration control devices *PhD Thesis* The Ohio State University
[31] Scheidler J J and Dapino M J 2016 Mechanically induced magnetic diffusion in cylindrical magnetoelastic materials *J. Magn. Magn. Mater.* **397** 233–9
[32] Etrema Products, Inc 2005 Terfenol-D data sheet available online www.etrema.com/terfenol-d/
[33] Zhao X and Lord D G 2006 Application of the Villari effect to electric power harvesting *J. Appl. Phys.* **99** 08M703
[34] Engdahl G and Bergqvist A 1996 Loss simulations in magnetostrictive actuators *J. Appl. Phys.* **79** 4689–91
[35] Scheidler J J, Asnani V M, Deng Z and Dapino M J 2015 Dynamic characterization of Galfenol *Proc. SPIE* **9432** 94320J
[36] ASTM International 2008 ASTM E 467—08: Standard practice for verification of constant amplitude dynamic forces in an axial fatigue testing system www.astm.org/Standards/E467.htm
[37] Fukada E, Date M and Sekigawa K 2003 Vibration control by magnetostrictive actuator coupled with negative inductance circuits *Japan. J. Appl. Phys.* **42** 7124